Electrochemical Diazidation of Alkenes Catalyzed by Manganese Porphyrin Complexes with Second-Sphere Hydrogen-Bond Donors

Luiz F. T. Novaes,† Yi Wang,† Jinjian Liu,† Xavier Riart-Ferrer,‡, Wan-Chen Cindy Lee,‡ Niankai Fu,†,§ Justin S. K. Ho,† X. Peter Zhang,*,‡ and Song Lin*,†

†Department of Chemistry and Chemical Biology, Cornell University, Ithaca, New York 14853, United States ‡Department of Chemistry, Merkert Chemistry Center, Boston College, Chestnut Hill, Massachusetts 02467, United States KEYWORDS: Electrochemistry, Electrocatalysis, Organic azide, Vicinal diamine, Metalloporphyrin

ABSTRACT: In this work, we report manganese porphyrin complexes for the electrocatalytic vicinal diazidation of alkenes with sodium azide. This protocol shows improved practicality over our previous work using $MnBr_2$ catalysis in the following aspects: (1) It requires substantially lower catalyst loading (as low as 0.3 mol%), which reduces the formation of metal azide complexes and simplifies product purification; (2) The introduction of a neutral aqueous buffer prevents the generation of toxic hydrazoic acid, contributing to a safer experimental procedure; (3) The catalytic system displays improved reactivity towards unactivated terminal alkenes. Mechanistic studies support the roles of second-sphere hydrogen-bond donors in stabilizing key reaction intermediates.

Organic azides find broad applications in many areas of chemistry such as chemical biology, materials science, and organic synthesis. Vicinal diazides are a particularly interesting class of compounds, serving as precursors to vicinal diamines, a ubiquitous structural motif found in numerous medicinally relevant molecules as well as ligands in metal-based catalysis. The construction of vicinal diazides from simple alkenes has the potential to accelerate the discovery and preparation of functional molecules. Indeed, this transformation has been achieved using various chemical methods, which however frequently rely on the use of stoichiometric amounts of oxidants.

With the objective of improving the practicality and reducing the environmental impact of this transformation, we have previously developed a general electrochemical approach for alkene diazidation using a catalytic amount of MnBr₂ (Scheme 1A).⁷ Electricity was used as a traceless carrier of redox equivalents to turn over the catalyst and generate reactive intermediates, and H⁺ was employed as an innocuous terminal oxidant, generating H2. Select examples of vicinal diazide products have been subjected to testing on their decomposition profile and impact sensitivity (vide infra), providing a guideline for safely handling these compounds.8 In addition, tandem procedures have been advanced to reduce diazides to the corresponding vicinal diamines with minimal purification of the intermediates.8,9 Despite showing key improvements over the prior art, this methodology also presents salient limitations. For example, scaling up the reaction can pose a safety challenge due to the use of acetic acid as the H⁺ source, leading to the formation of toxic and hazardous hydrazoic acid. 10 In addition, because this reaction

does not require an exogenous ligand, the structure of the active catalyst remains difficult to identify, making systematic tuning of reactivity challenging. To address these issues, we developed a second-generation electrochemical diazidation method used an aminoxyl radical catalyst, CHAMPO, under neutral conditions (Scheme 1B).¹¹ However, a high catalyst loading is required to achieve high conversion, and the reaction medium gradually becomes alkaline due to the cathodic reduction of water, which could limit compatibility with base-sensitive substrates.

To further expand the practicality and safety factors of electrochemical diazidation, we sought a catalytic system that would be compatible with a neutral medium, could be carried out with reduced catalyst loading and without perchlorate salts, and could be systematically modified to address substrate limitations in our previous methods. 12 We identified that manganese porphyrin complexes are ideal catalysts towards meeting the above-mentioned aims (Scheme 1C). Porphyrins with D_{2h} - and D_2 -symmetry can be synthesized in a modular fashion with easy variation of the peripheral substituents, allowing for tuning of steric, electronic, and chiral environment.¹³ Indeed, fully symmetrical Mn porphyrins have been used for the azidation of C-H bonds via chemical oxidation.¹⁴ However, structural tuning of porphyrin by introducing second-sphere functional groups has not been systematically investigated in such systems.

Scheme 1. Electrochemical Strategies for Accessing 1,2-Diazides

For developments in chemical diazidation, see references 6a-6f.

(A) Electrochemical Diazidation Catalyzed by MnBr₂

(B) Electrochemical Diazidation Catalyzed by Aminoxyl

(C) This work: Electrochemical Diazidation Catalyzed by Mn-porphyrin



- Improved safety and practicality Suppressed HN₃ formation, reduced metal-N₃ formation and eliminated LiClO₄ use
- Reduced catalyst loading 0.5 mol%
- Modular and tunable ligand
 Improved reactivity for unactivated alkenes

Several sets of screening experiments led us to identify a manganese(III) complex of D_{2h}-symmetric amidoporphyrin, [Mn(L1)Cl] (L1 = $3,5-Di^tBu-IbuPhyrin$), as an excellent electrocatalyst for the diazidation of alkenes (Table 1). Using 4-tert-butystyrene 1 as a model substrate and NaN3 as the nitrogen source, 1 mol% [Mn(L1)Cl] promotes the formation of diazide **2** in excellent yield under constant voltage (U_{cell} = 2.1 V), in a mixture of MeCN and neutral phosphate buffer solution without an additional electrolyte (entry 1). [Mn(L1)Cl] was readily synthesized in four steps from pyrrole and 2,6dibromobenzaldehyde. 15 In the absence of an electrocatalyst, a background reaction took place to give 24% yield of diazide 2 in addition to undesired products such as 4-tBubenzaldehyde and azidohydrin (entry 2). Using simple MnBr₂ the optimal catalyst in our first-generation diazidation method7—instead of [Mn(L1)Cl] only furnished 31% yield of the desired product even at 5 mol% catalyst loading (entry 3) in addition to side products. In this case, the Mn salt predominantly remains in the aqueous phase and the characteristic brown color of the key Mn(III)-N₃ intermediate was barely visible during the reaction.

We surveyed several additional Mn^{III} porphyrin catalysts and identified that [Mn(L1)Cl] is particularly reactive under the optimal conditions. Commercially available manganese porphyrins, such as [Mn(TPP)CI] (TPP = tetraphenylporphyrin) and [Mn(TMP)Cl] (TMP = tetramesitylporphyrin), gave substantially lower yields upon full conversion of the alkene (entries 4 and 5). We also evaluated [Mn(L2)Cl] with the amide groups replaced by Br, but this catalyst did not provide nearly as high yield as [Mn(L1)Cl] (entry 6). Thus, we hypothesize that the amide groups play an important functional role in this reaction likely by stabilizing key Mn-N3 intermediates via hydrogen-bonding interactions (vide infra). Notably, we were able to lower the loading of [Mn(L1)Cl] to 0.5 mol% or 0.3 mol% with only a small loss in yield (entries 7 and 8). Reactions with 0.5 mol% or higher catalyst loading resulted in very clean conversion of the alkene to diazide 2.

The role of the phosphate buffer is to provide a conducting medium while also neutralizing any bases (OH⁻) generated simultaneously from the reduction of H⁺ on the cathode. Replacing the buffer with pure H₂O resulted in lower yields with side product formation (e.g., 4-^tBu-benzaldehyde and azidohydrin) (entry 9), and the addition of an organic soluble electrolyte TBABF₄ did not provide any improvement (entry 10). Measurement of the aqueous phase pH post-electrolysis showed the solution was significantly basified (pH > 11), which may have led to catalyst degradation, while under optimal condition (entry 7) the pH post-electrolysis remained at 7.

Acetone as the solvent (entry 11) or co-solvent (entry 12) provided similar yields when compared to the optimal conditions, which could be applied for substrates with limited solubility in MeCN. The current optimal system using a Mn porphyrin catalyst and a buffer solution allowed us to circumvent the generation of hazardous hydrazoic acid, thus significantly improving the safety factor and practicality of the protocol while maintaining the simplicity and mildness of the reaction conditions.

Table 1. Reaction Optimization^a

Entry	Catalyst	Solvent I	Electrolyte	H ⁺ source	Yield ^c
1	[Mn(L1)Cl]	MeCN	-	Buffer ^b	87%
2	-	MeCN	-	Buffer ^b	24%
3	MnBr ₂ •4H ₂ O (5 mol%)	MeCN	-	Buffer ^b	31%
4	[Mn(TPP)CI]	MeCN	-	Buffer ^b	40%
5	[Mn(TMP)CI]	MeCN	-	Buffer ^b	44%
6	[Mn(L2)Cl]	MeCN	-	Buffer ^b	48%
7	[Mn(L1)CI] (0.5 mol%) MeCN	-	Buffer ^b	86%
8	[Mn(L1)Cl] (0.3 mol%)	MeCN	-	Buffer ^b	77%
9	[Mn(L1)Cl]	MeCN	-	H_2O	65%
10	[Mn(L1)Cl]	MeCN	TBABF ₄	H_2O	48%
11	[Mn(L1)Cl]	Acetone	-	Buffer ^b	85%
12	[Mn(L1)Cl]	MeCN/Acetone (2:1)	-	Buffer ^b	86%

 $^{\rm a}$ Reaction conditions: **1** (0.2 mmol, 1 equiv), Mn-catalyst (1 mol%), NaN $_{\rm 3}$, (5 equiv), electrolyte (0.4 mmol), solvent (3 mL), H $^+$ source (1 mL), C felt anode, Pt plate cathode, undivided cell, constant voltage $U_{cell}=2.1$ V, all reactions were conducted until full conversion of alkene **1**. $^{\rm b}$ Phosphate buffer (0.5 M K $_{\rm 2}$ HPO $_{\rm 4}$ + 0.5 M KH $_{\rm 2}$ PO $_{\rm 4}$). $^{\rm c}$ NMR yield using 1,3,5-trimethoxybenzene as standard.

Under the optimal conditions, we explored the generality of this method with structurally diverse alkenes (Table 2). Diazides derived from styrenes with different substitutions and electronic properties could be obtained in good yields (2–7). To ensure full solubility of *E*- and *Z*-stilbene, we employed acetone as a co-solvent, and this approach was also applied to the synthesis of diazides 8 and 14.

Unactivated alkenes are also suitable substrates but furnished the diazides in lower yields at room temperature

likely due to catalyst degradation. 16 Nonetheless, by simply cooling the reaction to 0 °C, the high efficiency could be restored, furnishing compounds 8-20 in high yields. Products 8-11 showcase the reactivity across different substitution patterns of alkenes (e.g., monosubstituted; 1,1- and 1,2disubstituted; and trisubstituted). For compound 13, side products from S_N2 or E2 reaction of the tosylate group was not observed, suggesting that the presence of water likely reduces the nucleophilicity of azide via H-bonding interactions. 17 Free alcohol was well tolerated (14) without observing the corresponding aldehyde or carboxylic acid side products. Electron-deficient methyl cinnamate reacted smoothly to furnish diazide 15 at 0 °C. Various nitrogen-containing functional groups commonly encountered in medicinal chemistry, 18 such as amide, carbamate, urea, benzimidazole, and indole, were all compatible with this methodology (16-20). Notably, this improved catalytic system is more reactive than the original MnBr₂ system, ⁷ as the reaction requires 10-20 times less catalyst loading and does not require heating to achieve high yields for electronically unactivated alkenes (e.g., 11, 16, and 18) or deactivated alkene (15). Finally, we carried out hazard assessment for handling diazide 7 (see SI).19

Table 2. Substrate Scope^a

^aReaction conditions: Alkene (0.2 mmol, 1 equiv), Mn-catalyst (0.5 mol%), NaN₃, (5 equiv), MeCN (3 mL), Phosphate buffer (0.5 M K₂HPO₄ + 0.5 M KH₂PO₄, 1 mL), C felt anode, Pt plate cathode, undivided cell, constant voltage U_{cell} = 2.1 V. ^bMeCN was replaced by a mixture of MeCN/acetone (2:1, 3 mL).

Ligand L1 provides a significantly higher yield and cleaner reaction than other types of porphyrins (see Table 1), suggesting that the H-bonding interactions exerted by the amide groups play important roles. Similar noncovalent interactions have been shown to facilitate the stabilization and activation of structurally analogous Co(L1)-nitrene radical intermediates in aziridination of styrenes. 15 In addition, second-sphere H-bonds have been shown to facilitate electrocatalytic CO₂ reduction by metal porphyrins.²⁰ We envision that in the current system, the azide group bound to the Mn center could engage in dual H-bonding with the N-H groups in a similar fashion. UV-vis titration of [Mn(L1)Cl] with NaN₃ revealed quantitative formation of a new manganese complex containing one azide ligand (see SI for details). Attempts to isolate this complex for structural elucidation have been thus far unsuccessful.²¹

To probe the structure of [Mn(L1)N₃], we performed density functional theory (DFT) calculations at the B3LYP-D3(BJ)/def2-SVP level. To reduce the computational expenses, the isopropyl and *tert*-butyl groups of L1 were replaced by hydrogen atoms (L3). Electronic structure calculations indicate that [Mn^{III}(L3)N₃] exhibits a quintet ground state. Two N–H···N H-bonds between the amide and azidyl groups were identified and further confirmed by the Quantum Theory of Atoms in Molecules (Figure 1A). The N–H···N3 (N3 = distal nitrogen atom of the Mn-bound N₃) H-bond is shorter and stronger than the N–H···N1 (N1 = Mn-bound nitrogen atom) H-bond.

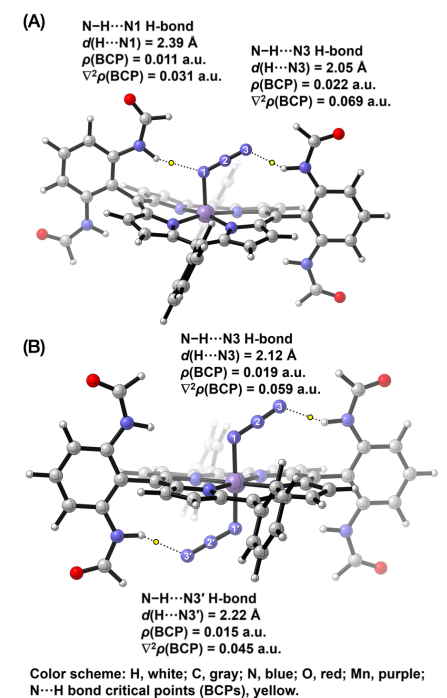


Figure 1. Optimized geometries for (A) [Mn(L3)N₃] (S = 2) and (B) [Mn(L3)(N₃)₂] (S = 3/2) at the B3LYP-D3(BJ)/def2-SVP level. ρ = electron density. $\nabla^2 \rho$ = Laplacian of electron density.

We further investigated the structure of the anodically generated diazidomanganese(IV) intermediate (Figure 1B), whose presence has been postulated in the literature²⁹ and supported by our own cyclic voltammetry data (*vide infra*). Topological analysis supports the existence of H-bonds

between the second-sphere amide groups and the Mn-bound azides, which likely stabilize the key intermediates.

We conducted cyclic voltammetry analysis to elucidate the active catalytic species in the reaction (Figure 2). In MeCN, the oxidation of tetrabutylammonium azide (TBAN₃), a soluble source of azide anion, shows an oxidation wave at $E_{\rm p/2}$ = +453 mV (vs. Fc^{+/0}), with an onset potential of +165 mV. The complex [Mn(L1)Cl] alone only exhibits oxidation above +600 mV, with two overlapping features that correspond to two sequential 1-electron oxidation events of [Mn(L1)Cl] likely accompanied by ligand addition (e.g., MeCN). After mixing [Mn(L1)Cl] and TBAN₃, the redox wave of [Mn(L1)Cl] at +800 mV disappeared and a new redox peak at $E_{1/2}$ = +155 mV appeared. We attribute this peak to the oxidation of an incipient manganese-azide complex, plausibly [Mn(L1)N₃]. Notably, ligand exchange from Cl⁻ to N₃⁻ significantly lowered the oxidation potential of the Mn^{III} complex by >600 mV.

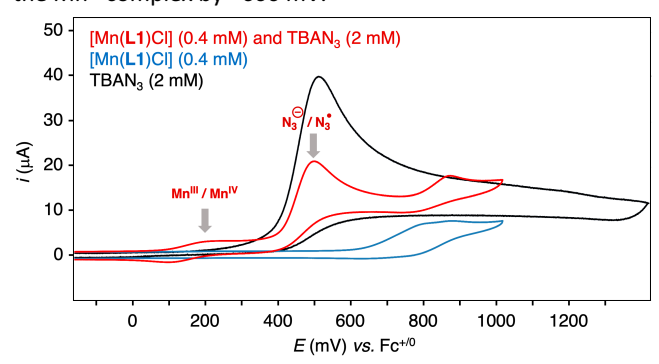


Figure 2. Cyclic voltammetry studies, MeCN (solvent), LiClO₄ (0.1 M), scan rate = 30 mV/s, glassy carbon working electrode.

We carried out the electrolysis under the optimal conditions using alkene ${\bf 1}$ and monitored the anodic potential. The potential raised from +230 mV to +420 mV (vs. Fc^{+/0}) through the course of the reaction, which is enough to oxidize both free N_3^- and the putative [Mn(L1)N $_3$] complex. Thus, both direct and Mn-mediated azide oxidation are considered as possible pathways to initiate alkene diazidation.

Experimental data together with related literature reports^{30,31} suggested that our reaction proceeds through a formally Mn^{III}/Mn^{IV} cycle. Taken together, we propose the following reaction mechanism via anodically coupled electrolysis (Scheme 2).³² Upon reaction of [Mn(L1)Cl] with N₃⁻ to form [Mn(L1)N₃], anodic oxidation of [Mn(L1)N₃] followed by fragmentation of the resultant [Mn(L1)(N₃)₂] gave rise to a free azidyl radical. Alternatively, direct oxidation of N₃⁻ can also lead to the same outcome. The incipient azidyl radical adds to alkene I to form transient radical II.³³ Given crosscoupling of two transient radicals is statistically disfavored,³⁴ the second C–N formation proceeds through azidyl transfer from anodically generated [Mn(L1)(N₃)₂] to II, thus delivering diazide III.

The mechanistic insights suggest that introduction of chiral information on the porphyrin ligand could enable the development of an asymmetric version of this method. Thus, Mn^{III} complexes of D_2 -symmetric chiral amidoporphyrins³⁵ were explored as catalysts in the diazidation of 4-tert-butystyrene (1) (Table 3). While [Mn(L4)CI] (L4 = 3,5-Di⁴Bu-

ChenPhyrin) gave diazide **2** in a racemic form, [Mn(**L5**)Cl] (**L5** = 2,6-DiMeo-ChenPhyrin) containing 2,6-dimethoxyphenyl groups instead of 3,5-di-*tert*-butylphenyl groups provided low but significant asymmetric induction (13% e.e.), implying that structurally tuning of the porphyrin ligand could impact the stereoselectivity of the electrochemical diazidation. This preliminary result indicates that the second azidyl transfer from a manganese azide complex is a plausible pathway.

Scheme 2. Proposed Mechanism

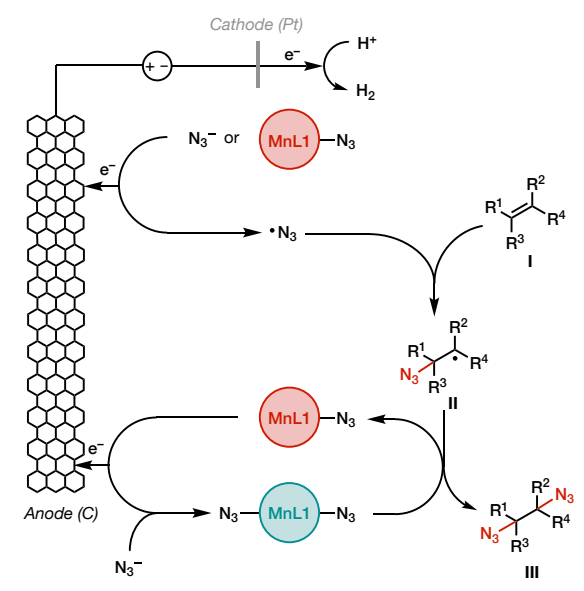


Table 3. Enantioselective Diazidation of 4-tert-Butylstyrene^a

^aReaction conditions: 1 (0.2 mmol, 1 equiv), Mn-catalyst (1 mol%), NaN₃, (5 equiv), MeCN (3 mL), Phosphate buffer (0.5 M K₂HPO₄ + 0.5 M KH₂PO₄, 1 mL), C felt anode, Pt plate cathode, undivided cell, constant voltage $U_{cell} = 2.1$ V.

In conclusion, we reported electrocatalytic diazidation of alkenes mediated by a new manganese porphyrin complex. A safer protocol was developed using an aqueous phosphate buffer, which suppressed the formation of toxic hydrazoic acid and circumvented the use of perchlorate electrolytes. This methodology proved to be general across a diverse range of alkenes, showing improved reactivity for unactivated alkenes vis-à-vis our previous MnBr₂-catalyzed system. Mechanistic investigation revealed that second-sphere H-bonding interactions stabilize key metal-azido intermediates and suggested the possibility of asymmetric catalysis, which will be the focus of our ongoing work.

ASSOCIATED CONTENT

AUTHOR INFORMATION

Corresponding Author

*songlin@cornell.edu

*peter.zhang@bc.edu

ORCID

Luiz F. T. Novaes: 0000-0003-1209-2865

Yi Wang: 0000-0001-5762-5958

Wan-Chen Cindy Lee: 0000-0002-2433-7404 X. Peter Zhang: 0000-0001-7574-8409 Song Lin: 0000-0002-8880-6476

Notes

The authors declare no competing financial interest.

Supporting Information

The Supporting Information is available free of charge on the ACS Publications website.

Experimental procedures, characterization data, and computational details (PDF)

ACKNOWLEDGMENT

Financial support was provided by NSF (CHE-1751839 to S.L. and CHE-2154885 to X.P.Z). S.L. thanks the Dreyfus Foundation for a Teacher-Scholar Award and BMS for an Unrestricted Grant in Synthetic Organic Chemistry. This study made use of the NMR facility supported by NSF (CHE-1531632 and CHE-2117246). LFTN acknowledges CNPq for a postdoctoral fellowship (National Council for Scientific and Technological Development, #200598/2019-8). The authors would also like to thank Professor Davin Piercey and Shannon Elyse Creegan of Purdue University for carrying out the impact and friction sensitivity test, as well as Anthony Condo Jr. of the Cornell Center for Materials Research (CCMR) for carrying out the DSC analysis.

Present Address

IIX.R.F.: GlaxoSmithKline, Collegeville, Pennsylvania 19426, United States

§N.F.: Key Laboratory of Molecular Recognition and Function, Institute of Chemistry, Chinese Academy of Sciences, Beijing 100190, China

REFERENCES

- Sletten, E. M.; Bertozzi, C. R. From Mechanism to Mouse: A Tale of Two Bioothogonal Reactions. Acc. Chem. Res. 2011, 44, 666-676.
- (2) (a) Zhang, G.; Chen, G.; Li, J.; Sun, S.; Luo, Y.; Li, X. High Azide Content Hyperbranched Star Copolymer as Energetic Materials. *Ind. Eng. Chem. Res.* 2018, 57, 13962-13972. (b) Qin, A.; Lam, J. W. Y.; Jim, C. K. W.; Zhang, L.; Yan, J.; Häussler, M.; Liu, J.; Dong, Y.; Liang, D.; Chen, E.; Jia, G.; Tang, B. Z. Hyperbranched Polytriazoles: Click Polymerization, Regioisomeric Structure, Light Emission, and Fluorescent Patterning. *Macromolecules* 2008, 41, 3808-3822.
- (3) For selected total synthesis of alkaloids containing organic azides as intermediates, see: (a) Frost, J. R.; Pearson, C. M.; Snaddon, T. N.; Booth, R. A.; Turner, R. M.; Gold, J.; Shaw, D. M.; Gaunt, M. J.; Ley, S. V. Callipeltosides A, B and C: Total Syntheses and Structural Confirmation. Chem. Eur. J. 2015, 21,

- 13261-13277. (b) Seiple, I. B.; Shun, S.; Young, I. S.; Nakamura, A.; Yamaguchi, J.; Jørgensen, L.; Rodriguez, R. A.; O'Malley, D. P.; Gaich, T.; Köck, M.; Baran, P. S. Enantioselective Total Syntheses of (-)-Palau'amine, (-)-Axinellamines, and (-)-Massadines. *J. Am. Chem. Soc.* **2011**, *133*, 14710-14726. (c) Cakmak, M.; Mayer, P.; Trauner, D. An Efficient Synthesis of Loline Alkaloids. *Nat. Chem.* **2011**, *3*, 543-545.
- (4) (a) For a recent overview of Tamiflu history and synthetic approaches, see: Sagandira, C. R.; Mathe, F. M.; Guyo, U.; Watts, P. The evolution of Tamiflu synthesis, 20 years on: Advent of enabling technologies the last piece of the puzzle? Tetrahedron, 2020, 76, 131440. (b) Saibabu Kotti, S. R. S.; Timmons, C.; Li, G. Vicinal diamino functionalities as privileged structural elements in biologically active compounds and exploitation of their synthetic chemistry. Chem. Biol. Drug Des. 2006, 67, 101- 114. (c) Viso, A.; Fernández de la Pradilla, R.; Tortosa, M.; García, A.; Flores, A. Update 1 of: α,β-Diamino Acids: Biological Significance and Synthetic Approaches. Chem. Rev. 2011, 111, PR1-PR42.
- (5) (a) Chen, M. S.; White, M. C. A Predictably Selective Aliphatic C-H Oxidation Reaction for Complex Molecule Synthesis. Science 2007, 318, 783-787. (b) Zhang, W.; Loebach, J. L.; Wilson, S. R.; Jacobsen, E. N. Enantioselective Epoxidation of Unfunctionalized Olefins Catalyzed by Salen Manganese Complexes. J. Am. Chem. Soc. 1990, 112, 2801-2803.
- (a) Minisci, F.; Galli, R. Influence of The Electrophilic Character on The Reactivity of Free Radicals in Solution Reactivity of Alkoxy, Hydroxy, Alkyl and Azido Radicals in Presence of Olefins. Tetrahedron Lett. 1962, 3, 533-538. (b) Magnus, P.; Lacour, J.; Evans, P. A.; Roe, M. B.; Hulme, C. Hypervalent lodine Chemistry: New Oxidation Reactions Using the Iodosylbenzene-Trimethylsilyl Azide Reagent Combination. Direct α - and β -Azido Functionalization of Triisopropylsilyl Enol Ethers. J. Am. Chem. Soc. 1996, 118, 3406-3418. (c) Snider, B. B.; Lin, H. An Improved Procedure for the Conversion of Alkenes and Glycals to 1,2-Diazides Using Mn(OAc)₃·2H₂O in Acetonitrile Containing Trifluoroacetic Acid. Synth. Commun. 1998, 28, 1913-1922. (d) Yuan, Y. A.; Lu, D. F.; Chen, Y. R.; Xu, H. Iron-Catalyzed Direct Diazidation for a Broad Range of Olefins. Angew. Chem., Int. Ed. 2016, 55, 534-538. (e) Peng, H.; Yuan, Z.; Chen, P.; Liu, G. Palladium-Catalyzed Intermolecular Oxidative Diazidation of Alkenes. Chin. J. Chem. 2017, 35, 876-880. (f) Shen, S.-J.; Zhu, C.-L.; Lu, D.-F.; Xu, H. Iron- Catalyzed Direct Olefin Diazidation via Peroxyester Activation Promoted by Nitrogen-Based Ligands. ACS Catal. 2018, 8, 4473-4482.
- (7) Fu, N; Sauer, G. S.; Saha, A.; Loo, A.; Lin, S. Metal-Catalyzed Electrochemical Diazidation of Alkenes. *Science* 2017, 357, 575-579.
- (8) Zhu, H.-T.; Arosio, L.; Villa, R.; Nebuloni, M.; Xu, H. Process Safety Assessment of the Iron-Catalyzed Direct Olefin Diazidation for the Expedient Synthesis of Vicinal Primary Diamines. Org. Process Res. Dev. 2017, 21, 2068-2072.
- (9) Ho, J. S. K.; Chang, Y.; Novaes, L. F. T.; Siu, J. C.; Lin, S. Cornell University, Ithaca, NY. Unpublished work, 2022.
- (10) Treitler, D. S.; Leung, S. How Dangerous Is Too Dangerous? A Perspective on Azide Chemistry. J. Org. Chem. 2022, 87, 11293-11295.
- (11) (a) Siu, J. C.; Parry, J. B.; Lin, S. Aminoxyl-Catalyzed Electrochemical Diazidation of Alkenes Mediated by a Metastable Charge-Transfer Complex. *J. Am. Chem. Soc.* **2019**, *141*, 2825-2831. (b) Nelson, H.; Siu. J. C.; Saha, A.; Cascio, D.; Wu, S.-B.; Lu, C.; Rodriguez, J. A.; Houk, K. N.; Lin, S. Isolation and X-ray Crystal Structure of an Electrogenerated TEMPO—N₃ Charge-Transfer Complex. *Org. Lett.* **2021**, *23*, 454-458.
- (12) During the preparation of this manuscript, a related work was published: Cai, C.-Y.; Zheng, Y.-T.; Li, J.-F.; Xu, H.-C. Cu-

- Electrocatalytic Diazidation of Alkenes at ppm Catalyst Loading. J. Am. Chem. Soc. 2022, 144, 11980-11985.
- (13) For representative examples, see: (a) Hu, Y.; Lang, K.; Li, C.; Gill, J. B.; Kim, I.; Lu, H.; Fields, K. B.; Marshall, M.; Cheng, Q.; Cui, X.; Wojtas, L.; Zhang, X. P. Enantioselective Radical Construction, of 5-Membered Cyclic Sulfonamides by Metalloradical C-H Amination. J. Am. Chem. Soc. 2019, 141, 18160-18169. (b) Lang, K.; Torker, S.; Wojtas, L.; Zhang, X. P. Asymmetric Induction and Enantiodivergence in Catalytic Radical C-H Amination via Enantiodifferentiative H-Atom Abstraction and Stereoretentive Radical Substitution. J. Am. Chem. Soc. 2019, 141, 12388-12396. (c) Lang, K.; Yang, H.; Lee, W.-C. C.; Zhang, X. P. "Combined Radical and Ionic Approach for The Enantioselective Synthesis of β-Functionalized Amines from Alcohols" Nat. Synth. 2022, 1, 548-557. (d) Lang, K.; Li, C.-Q.; Kim, I.; Zhang, X. P. "Enantioconvergent Amination of Racemic Tertiary C-H Bonds" J. Am. Chem. Soc. 2020, 142, 20902-20911. (e) Jin, L.-M.; Xu, P.; Xie, J.-J.; Zhang, X. P. "Enantioselective Intermolecular Radical C-H Amination" J. Am. Chem. Soc. 2020, 142, 20828-20836.
- (14) Huang, X.; Bergsten, T. M.; Groves, J. T. Manganese-Catalyzed Late-Stage Aliphatic C–H Azidation. *J. Am. Chem. Soc.* **2015**, *137*, 5300-5303.
- (15) Ruppel, J. V.; Jones, J. E.; Huff, C. A.; Kamble, R. M.; Chen, Y.; Zhang, X. P. A Highly Effective Cobalt Catalyst for Olefin Aziridination with Azides: Hydrogen Bonding Guided Catalyst Design. Org. Lett. 2008, 10, 1995–1998.
- (16) For diazidation of unactivated alkenes at room temperature, we observed discoloration (dark green to light amber) of the reaction mixture after 0.2-0.5 F/mol, indicating catalyst degradation. When the reaction was conducted at 0 °C, the characteristic dark green color remained for the majority of the reaction, and partial discoloration was observed towards the end of the electrolysis.
- (17) Nucleophilic substitution of primary tosylates with NaN₃ has been reported under anhydrous conditions. (a) Olsson, C. R.; Payette, J. N.; Cheah, J. H.; Movassaghi, M. Synthesis of Potent Cytotoxic Epidithiodiketopiperazines Designed for Derivatization. *J. Org. Chem.* 2020, 85, 4648-4662. (b) Wessig, P.; Freyse, D.; Schuster, D.; Kelling, A. Fluorescent Dyes with Large Stokes Shifts Based on Benzo[1,2-d:4,5-d']bis([1,3]dithiole) ("S⁴-DBD Dyes"). *Eur. J. Org. Chem.* 2020, 2020, 1732-1744. (c) Furman, B.; Dziedzic, M. An Efficient Route to 4-(Substituted benzyl)piperidines. *Tetrahedron Lett.* 2003, 44, 8249-8252.
- (18) (a) Vitaku, E.; Smith, D. T.; Njardarson, J. T. Analysis of the Structural Diversity, Substitution Patterns, and Frequency of Nitrogen Heterocycles among U.S. FDA Approved Pharmaceuticals. J. Med. Chem. 2014, 57, 10257-10274. (b) Roughley, S.; Jordan, A. M. The Medicinal Chemist's Toolbox: An Analysis of Reactions Used in the Pursuit of Drug Candidates. J. Med. Chem. 2011, 54, 3451-3479.
- (19) Diazide 7 shows an onset decomposition temperature at 202 °C using differential scanning calorimetry. It is shown to be insensitive to impact but sensitive to friction, although no detonation was observed during the measurements. Although our measurements suggest that diazide 7 can be handled safely at room temperature and that no accident has taken place in our laboratory, it is important to note that the decomposition profile and sensitivity of other diazides shown in this manuscript have not been tested at the moment, and that appropriate safety practices should be observed when handling all diazide products.
- (20) For representative examples, see: (a) Derrick, J. S.; Loipersberger, M.; Nistanaki, S. K.; Rothweiler, A. V.; Head-Gordon, M.; Nichols, E. M.; Chang, C. J. Templating Bicarbonate in the Second Coordination Sphere Enhances

- Electrochemical CO₂ Reduction Catalyzed by Iron Porphyrins. *J. Am. Chem. Soc.* **2022**, *144*, 11656-11663. (b) Costentin, C.; Drouet, S.; Robert, M.; Savéant, J.-M. A Local Proton Source Enhances CO₂ Electroreduction to CO by a Molecular Fe Catalyst. *Science* **2012**, *338*, 90-94.
- (21) Manganese porphyrin complexes containing azide as ligand have been analyzed by X-ray previously, for an example, see: Day, V. W.; Stults, B. R.; Tasset, E. L.; Day, R. O.; Marianelli, R. S. Coordination Geometries of High-Spin Manganese(III) Porphyrins and Their Synthetic Intermediates. J. Am. Chem. Soc. 1974, 96, 2650-2652.
- (22) Frisch, M. J.; Trucks, G. W.; Schlegel, H. B.; Scuseria, G. E.; Robb, M. A.; Cheeseman, J. R.; Scalmani, G.; Barone, V.; Petersson, G. A.; Nakatsuji, H.; Li, X.; Caricato, M.; Marenich, A. V.; Bloino, J.; Janesko, B. G.; Gomperts, R.; Mennucci, B.; Hratchian, H. P.; Ortiz, J. V.; Izmaylov, A. F.; Sonnenberg, J. L.; Williams-Young, D.; Ding, F.; Lipparini, F.; Egidi, F.; Goings, J.; Peng, B.; Petrone, A.; Henderson, T.; Ranasinghe, D.; Zakrzewski, V. G.; Gao, J.; Rega, N.; Zheng, G.; Liang, W.; Hada, M.; Ehara, M.; Toyota, K.; Fukuda, R.; Hasegawa, J.; Ishida, M.; Nakajima, T.; Honda, Y.; Kitao, O.; Nakai, H.; Vreven, T.; Throssell, K.; Montgomery, J. A. Jr.; Peralta, J. E.; Ogliaro, F.; Bearpark, M. J.; Heyd, J. J.; Brothers, E. N.; Kudin, K. N.; Staroverov, V. N.; Keith, T. A.; Kobayashi, R.; Normand, J.; Raghavachari, K.; Rendell, A. P.; Burant, J. C.; Iyengar, S. S.; Tomasi, J.; Cossi, M.; Millam, J. M.; Klene, M.; Adamo, C.; Cammi, R.; Ochterski, J. W.; Martin, R. L.; Morokuma, K.; Farkas, O.; Foresman, J. B.; Fox, D. J. Gaussian 16, Revision C.01; Gaussian, Inc.: Wallingford, CT, 2019.
- (23) (a) Lee, C.; Yang, W.; Parr, R. G. Development of the Colle–Salvetti Correlation-Energy Formula into a Functional of the Electron Density. *Phys. Rev. B* **1988**, *37*, 785-789. (b) Becke, A. D. Density-Functional Thermochemistry. III. The Role of Exact Exchange. *J. Chem. Phys.* **1993**, *98*, 5648-5652.
- (24) Grimme, S.; Ehrlich, S.; Goerigk, L. Effect of the Damping Function in Dispersion Corrected Density Functional Theory. J. Comp. Chem. 2011, 32, 1456-1465.
- (25) Weigend, F.; Ahlrichs, R. Balanced Basis Sets of Split Valence, Triple Zeta Valence and Quadruple Zeta Valence Quality for H to Rn: Design and Assessment of Accuracy. *Phys. Chem. Chem. Phys.* 2005, 7, 3297-3305.
- (26) Other popular functionals such as PBE0-D3(BJ)^{19,21} and M06²² gave similar results, see Supporting Information for details. For PBE0-D3(BJ), see: reference 19 and (a) Adamo, C.; Barone, V. Toward Reliable Density Functional Methods without Adjustable Parameters: The PBE0 Model. *J. Chem. Phys.* 1999, 110, 6158-6170. For M06, see: (b) Zhao, Y.; Truhlar, D. G. The M06 Suite of Density Functionals for Main Group Thermochemistry, Thermochemical Kinetics, Noncovalent Interactions, Excited States, and Transition Elements: Two New Functionals and Systematic Testing of Four M06-Class Functionals and 12 Other Functionals. *Theor. Chem. Acc.* 2008, 120, 215-241.
- (27) Lu, T.; Chen, F. Multiwfn: A Multifunctional Wavefunction Analyzer. J. Comput. Chem. 2012, 33, 580-592.
- (28) The "Quantum Theory of Atoms in Molecules" is a powerful tool to identify the presence of hydrogen bond interactions: Bader, R. F. W. Atoms in Molecules: A Quantum Theory; Clarendon Press: Oxford, 1994.
- (29) Legault, C. Y. CYLview, 1.0b; Université de Sherbrooke, 2009, http://www.cylview.org (accessed 2017-10-07).
- (30) Camenzind, M. J.; Hollander, F. J.; Hill, C. L. Synthesis, Characterization, and Ground Electronic State of the Unstable Monomeric Manganese(IV) Porphyrin Complexes Diazidoand Bis(isocyanato)(5,10,15,20tetraphenylporphinato)manganese (IV). Crystal and

- Molecular Structure of the Bis(isocyanato) Complex. *Inorg. Chem.* **1983**, *22*, 3776-3784.
- (31) Meyer, T. H.; Samanta, R. C.; Del Vecchio, A.; Ackermann, L. Mangana(III/IV)electro-catalyzed C(sp³)–H azidation. *Chem. Sci.* **2021**, *12*, 2890-2897.
- (32) Additional DFT calculations were conducted to gain further insights into the full catalytic mechanism. See Section 5 of SI.
- (33) Kinetics of azidyl addition to alkenes has been reported, see: Workentin, M. S.; Wagner, B. D.; Lusztyk, J.; Wayner, D. D. M. Azidyl Radical Reactivity. N₆. as a Kinetic Probe for the Addition Reactions of Azidyl Radicals with Olefins. *J. Am. Chem. Soc.* **1995**, *117*, 119-126.
- (34) Yan, M.; Lo, J. C.; Edwards, J. T.; Baran, P. S. Radicals: Reactive Intermediates with Translational Potential. *J. Am. Chem. Soc.* **2016**, *138*, 12692-12714.
- (35) Chen, Y.; Fields, K. B.; Zhang, X. P. Bromoporphyrins as Versatile Synthons for Modular Construction of Chiral Porphyrins: Cobalt-Catalyzed Highly Enantioselective and Diastereoselective Cyclopropanation. J. Am. Chem. Soc. 2004, 126, 14718–14719.

